ChemComm

COMMUNICATION

View Article Online
View Journal | View Issue

Cite this: *Chem. Commun.*, 2014, **50**, 15521

Received 12th October 2014,
Accepted 20th October 2014

DOI: 10.1039/c4cc08063g

www.rsc.org/chemcomm

High alkalinity boosts visible light driven H_2 evolution activity of g-C_3N_4 in aqueous methanol†

Po Wu,[ab] Jiarui Wang,[b] Jing Zhao,[b] Liejin Guo*[a] and Frank E. Osterloh*[b]

A high rate of 2.23 mmol h^{-1} g^{-1} (quantum efficiency of 6.67% at 400 nm) for visible light driven photocatalytic H_2 evolution can be achieved with g-C_3N_4 by alkalization of the solution to a pH of 13.3, due to accelerated transfer of photoholes to the sacrificial donor.

Hydrogen production from photocatalytic water splitting under sunlight is regarded as a possible solution to global energy and environmental problems resulting from fossil fuel consumption.[1] However, the design of efficient visible-light-responsive photocatalysts remains a great challenge.[2] Different from the widely studied inorganic semiconductors (mainly oxides),[3] graphitic carbon nitride (g-C_3N_4) has aroused great interest in recent years, due to the appropriate band edge potentials and ease of synthesis.[4] However, the efficiency of the material is too low for practical applications. Improved hydrogen evolution rate (HER) can be achieved by increasing the surface area in porous[5] or nanosheet[6] forms of g-C_3N_4, or by introducing internal junctions to promote charge separation.[7] Herein, we report that the solution pH is a significant factor for the activity of g-C_3N_4. High alkalinity boosts hydrogen evolution to 2.23 mmol h^{-1} g^{-1} under visible light and allows for a quantum efficiency of 6.67% (400 nm). These values exceed those previously reported for g-C_3N_4.[8–10] Based on electrochemical and photovoltage data, the high activity is a result of an increased thermodynamic driving force for hole transfer at high pH.

The g-C_3N_4 materials used for this study were synthesised by heating either dicyandiamide (D), urea (U), thiourea (T) or stoichiometric mixtures (UT, 1 : 1 weight ratio) at 520 °C, to yield D52, U52, T52 and UT52, respectively. X-ray diffraction (XRD) patterns and Fourier transform infrared (FTIR) spectra (Fig. S1 and S2, ESI†) agree with the literature data,[4,11] confirming the graphitic structure. Fig. 1 shows an absorption edge at about 450 nm for all the samples. The corresponding bandgap values can be obtained by the intercept of extended linear region in the Tauc plot (right inset).[12] They vary from 2.88 eV for D52 to 2.99 eV for U52. U52 has the largest band gap, which may be a result of quantum confinement.[13] This is supported by a longer interlayer distance revealed from the low-angle shifted XRD patterns of the material (Fig. S1, ESI†). For T52 and UT52, the absorption spectra show a shoulder extending to 600 nm, indicative of the presence of defect levels in the band gap. In accord with this, the yellow colour of these materials is slightly darker.

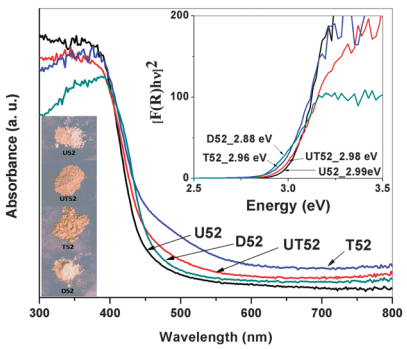

Fig. 1 UV-Vis absorption spectra, photos (left inset) and Tauc plots (right inset) of samples U52, UT52, T52 and D52.

In order to determine the photocatalytic hydrogen evolution activity of the materials, 1% (mass) of platinum was photodeposited on each sample. The visible light H_2 evolution from the resulting materials in aqueous methanol at pH 4.5 is shown in Fig. 2A. D52 had a better performance than U52 and T52, owing to less defects and better crystallization (Fig. S1, ESI†). UT52 supported a reaction rate of *ca.* 762 μmol h^{-1} g^{-1}, which is over four times higher than that of U52 and T52. It should be noted that, UT52 had less absorption than T52 (Fig. 1), but it had a significantly improved H_2 evolution activity, indicating that light absorption does not play the most important role in this photocatalytic reaction over g-C_3N_4. According to earlier studies,

[a] *International Research Center for Renewable Energy, State Key Laboratory of Multiphase Flow in Power Engineering, Xi'an Jiaotong University, No. 28 West Xianning Road, Xi'an, Shaanxi, 710049, P. R. China. E-mail: lj-guo@mail.xjtu.edu.cn; Fax: +86 02982669033; Tel: +86 02982663895*

[b] *Department of Chemistry, University of California, Davis, One Shields Avenue, Davis, CA, 95616, USA. E-mail: fosterloh@ucdavis.edu; Tel: +1 5307546242*

† Electronic supplementary information (ESI) available: Experimental details and Fig. S1–S7. See DOI: 10.1039/c4cc08063g

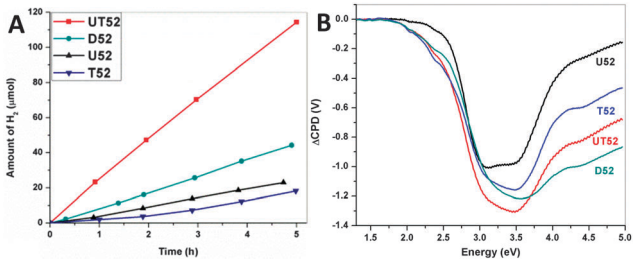

Fig. 2 (A) H_2 evolution from the samples (30 mg) in methanol (20 vol%) aqueous solution at pH = 4.5 under visible-light ($\lambda > 400$ nm) irradiation. The light power at the flask surface was 380 mW cm^{-2}. Samples were platinized with Pt (1 wt%) by photodeposition prior to testing. (B) SPV spectra of samples U52, UT52, T52 and D52. Films had average thickness of *ca.* 5 μm.

the enhanced performance of UT52 is attributed to a heterojunction in this material,[7] which arises from the use of two separate synthetic precursors, urea and thiourea. The compositional variations within the mixed g-C_3N_4 product generate a 0.1 eV conduction band (CB) offset and a 0.4 eV valence band (VB) offset that facilitate charge separation inside the material.[14] TEM images (Fig. S3, ESI†) seem to support this interpretation. They show a porous morphology for U52, a compact morphology for T52, and a combination of both for UT52.

To investigate the charge separation in g-C_3N_4, surface photovoltage (SPV) spectra were recorded for the entire series. In SPV, the surface potential of an illuminated particle film is measured as a function of photon energy.[15–17] The observed contact potential changes (ΔCPD) provide information about the majority carrier type, band gap, and other properties of the light absorber.[18–20] Measured spectra are shown in Fig. 2B. In all cases, negative voltages are observed, indicating majority carrier (electron) transfer from g-C_3N_4 into the ITO substrate. Small sub-gap photovoltage signals in particular for UT52, T52 and D52 can be attributed to defects, which is consistent with the UV-Vis spectra. The maximum photovoltage for these samples occur around 3.0–3.5 eV. Values lie between 1.01 V and 1.31 V, with the highest value observed for UT52. This suggests that charge separation and carrier lifetimes are improved in this material.

Recently, it has been reported that hydrogen evolution over $SrTiO_3$ could be improved significantly in alkaline solution.[21] To determine if a similar pH-dependence exists for g-C_3N_4, HER experiments for D52 were carried out at variable pH conditions. D52 was chosen because it is the most common form of g-C_3N_4 described in the literature. As shown in Fig. 3A, steady H_2 evolution is observed in all cases, with the evolution rate rising continuously as the pH value is increased. The highest activity is 1.56 mmol h^{-1} g^{-1} at pH = 13.3. The enhanced activity is not temporary but persistent for at least 15 h (Fig. S4, ESI†), yielding a turnover number of 1.82 based on 594 μmol evolved H_2. When the rates are plotted *versus* pH (Fig. 3B), a nearly exponential dependence between pH and the reaction rate is observed.

To rule out ionic strength as a factor, control experiments were conducted with KCl and NaOH electrolytes (Fig. 3C). These experiments show that KCl does not improve the reaction rate, whereas NaOH yields four times higher activity. This rate improvement is comparable to KOH, which shows that

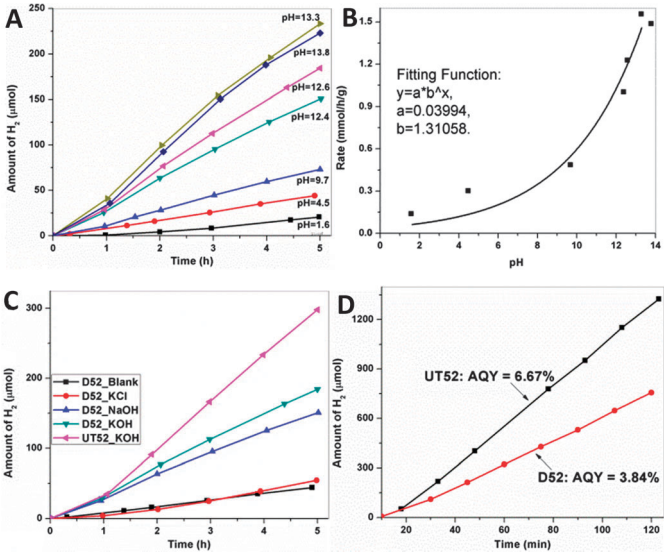

Fig. 3 (A) H_2 evolution from D52 (30 mg) in methanol (20 vol%) aqueous solution at different pH under visible light ($\lambda > 400$ nm) irradiation. (B) Plot of H_2 evolution rate *vs.* pH from (A) and the fitted exponential curve. (C) H_2 evolution in the presence of various electrolytes (0.4 M). (D) H_2 evolution over D52 or UT52 (30 mg) in basic (pH = 13.3) methanol (20 vol%) aqueous solution under 400 nm LED light irradiation for AQY calculation.

hydroxide concentration is the key parameter. A further boost of the activity could be achieved by replacing D52 with UT52. At pH = 13.3, the H_2 evolution rate is 2.23 mmol h^{-1} g^{-1}, approximately 14 times higher than that of U52 at pH 4.5. To determine the apparent quantum yield (AQY), H_2 evolution was performed under LED illumination (400 nm). From the rates in Fig. 3D, the AQY of D52 and UT52 were calculated to be 3.84% and 6.67%, respectively. This ranks among the highest activities reported for g-C_3N_4 (1.8–26.5%).[8–10,22] The total amount of H_2 generated over UT52 (1.32 mmol in 2 hours), exceeds the molar amount of g-C_3N_4 (0.33 mmol) by a factor of three, confirming the catalytic nature of the reaction. Additionally, FTIR spectra recorded for g-C_3N_4 before and after the reaction (Fig. S5, ESI†) do not show any photocatalyst degradation.

To elucidate the reasons for the increased activity, photocurrent scans were recorded on g-C_3N_4 films immersed in neutral or basic electrolyte solution, with or without added methanol (Fig. 4A and Fig. S6, ESI†). Under constant applied bias of 1.20 V (*vs.* RHE), a g-C_3N_4 film made of D52 only exhibits small chopped photocurrent of *ca.* 0.6 μA cm^{-2}. Upon addition of methanol the photocurrent increases to 1.2 μA cm^{-2}, and an additional increase to 4.2 μA cm^{-2} occurs after the addition of base to bring the pH to 12.8. This shows that hole transfer into the solution is promoted by the addition of methanol, especially at high pH. Photocurrent scans *versus* applied potential are shown in Fig. 4B. In 0.2 M Na_2SO_4 solution at pH = 5.6 (acidity due to CO_2 from air), a g-C_3N_4 film produces weak cathodic and anodic photocurrents when the applied potential was negative or positive of +0.38 V (*vs.* NHE). These currents are limited by slow charge transport in the g-C_3N_4 film, and by the absence of a space charge layer that could provide a photovoltage. When methanol (12.5 vol%) was added to the electrolyte, the cathodic

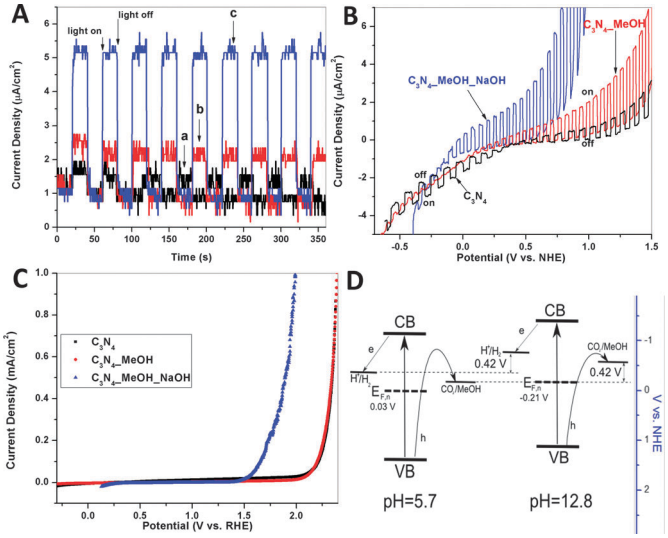

Fig. 4 (A) Photocurrent at 1.20 V (*vs.* RHE) for g-C_3N_4 film in aqueous NaOH solution (pH = 5.6, 5.7 and 12.8 for D52 [a], D52–MeOH [b] and D52–MeOH–NaOH [c], respectively) with or without 12.5 vol% methanol. A fiberoptics Xe light source (60 mW cm^{-2} at electrode) was used. (B) Photocurrent scans (positive to negative potential, 20 mV s^{-1}), (C) dark current scans in different solutions. (D) Energy diagrams of g-C_3N_4 at neutral and basic solution. The slightly lower pH (12.8) was used in the electrochemical experiments in order to prevent corrosion of the reference electrode at high pH.

photocurrent was suppressed and the anodic photocurrent was increased by 300%. This shows that methanol speeds up hole transfer from g-C_3N_4. Under these conditions the anodic photoonset potential can be taken as the quasi-Fermi level ($E_{F,n}$) of g-C_3N_4. The onset at +0.03 V (*vs.* NHE) is more negative than that without methanol (+0.38 V *vs.* NHE), in agreement with faster hole removal from g-C_3N_4, which reduces the positive charging of the material. The g-C_3N_4 flat-band and band-edge potentials, together with the methanol (and proton) redox potential, are shown in Fig. 4D.

Several changes in the system energetics occur upon raising the solution from 5.7 to 12.8 with NaOH. First, dark electrochemical scans on a g-C_3N_4 film electrode in aqueous methanol (Fig. 4C) show that the CH_3OH oxidation potential shifts cathodically by 0.54 V (*vs.* RHE) when the pH increases. Indeed, it is known that hydroxide facilitates proton abstraction from CH_3OH and promotes oxidation.[23] This pH change is expected to also move the quasi-Fermi level in g-C_3N_4 to more reducing values. However, the observed shift in the photoelectrochemical onset potential (Fig. 4B) from +0.03 V to −0.21 V (*vs.* NHE) is only 0.24 V, *i.e.* −0.032 per pH unit. This sub-Nernstian shift[24] can be explained by the acid–base chemistry of g-C_3N_4. It is well known that the surface of g-C_3N_4 is terminated by –NH/NH_2 groups[25] whose acidity is much lower than that of –OH typically found on the surface of metal oxides (pK_a = 38 for NH_3; pK_a = 14 for H_2O).[26,27] As a result, no significant deprotonation occurs at pH = 12.8, explaining the lack of negative charging and the sub-Nernstian Fermi level shift. This results in an increased driving force of 0.18 eV for hole transfer from g-C_3N_4 to methanol (Fig. 4D), and correspondingly higher charge transfer rate. This effect explains the higher photocatalytic hydrogen evolution rate resulting from alkalization. While the HER boost formally resembles that for photocatalytic hydrogen evolution from $SrTiO_3$,[21] the reason is fundamentally different. In the latter case, the enhancement at high pH is attributed to the generation of reactive hydroxyl radicals from hydroxide. This mechanism can be ruled out for g-C_3N_4 for lack of surface hydroxide. The model also provides a simple explanation for the high photocatalytic HER reported for g-C_3N_4 by Martin *et al.*[22] In that system, H_2 evolution tests were performed in 13 vol% triethanolamine solution in water. The pH of this solution was not stated in the paper but can be estimated as pH = 10.9, based on the pK_b = 6.24 for triethanolamine. That pH is close to the conditions employed here, and suggests the presence of a pH effect in that system.

In summary, we demonstrate a pH boost for the photocatalytic hydrogen evolution activity of g-C_3N_4 in solutions of sacrificial electron donors. In the case of UT52, high pH enables 2.23 mmol h^{-1} g^{-1} (AQY 6.67% at 400 nm) under visible light. The mechanism for this enhancement is revealed on the basis of surface photovoltage spectra and electrochemical measurements. It is mainly due to the increased driving force for photochemical methanol oxidation at high pH, which stems from the low acidity of the amine terminated g-C_3N_4 surface. This mechanism also explains the high activity for g-C_3N_4 in triethanolamine solution. Overall, this work promotes the understanding of photochemical charge transfer at non-oxide surfaces, as relevant to the conversion of sunlight into fuel.

We thank the Research Corporation for Science Advancement (Scialog award) and the National Science Foundation (NSF, CBET 1133099). Po Wu also thanks the State Scholarship Fund of the China Scholarship Council (CSC) and the National Natural Science Foundation of China (51323011 and 51121092).

Notes and references

1 F. E. Osterloh, *Chem. Soc. Rev.*, 2013, **42**, 2294.
2 X. B. Chen, S. H. Shen, L. J. Guo and S. S. Mao, *Chem. Rev.*, 2010, **110**, 6503.
3 F. E. Osterloh, *Chem. Mater.*, 2008, **20**, 35.
4 X. Wang, K. Maeda, A. Thomas, K. Takanabe, G. Xin, J. M. Carlsson, K. Domen and M. Antonietti, *Nat. Mater.*, 2009, **8**, 76.
5 Y. Wang, X. Wang and M. Antonietti, *Angew. Chem., Int. Ed.*, 2012, **51**, 68.
6 X. Zhang, X. Xie, H. Wang, J. Zhang, B. Pan and Y. Xie, *J. Am. Chem. Soc.*, 2013, **135**, 18.
7 F. Dong, Z. Zhao, T. Xiong, Z. Ni, W. Zhang, Y. Sun and W.-K. Ho, *ACS Appl. Mater. Interfaces*, 2013, **5**, 11392.
8 H. Yan, *Chem. Commun.*, 2012, **48**, 3430.
9 J. Hong, X. Xia, Y. Wang and R. Xu, *J. Mater. Chem.*, 2012, **22**, 15006.
10 Y.-S. Jun, J. Park, S. U. Lee, A. Thomas, W. H. Hong and G. D. Stucky, *Angew. Chem.*, 2013, **125**, 11289.
11 S. Martha, A. Nashim and K. M. Parida, *J. Mater. Chem. A*, 2013, **1**, 7816.
12 S. Datta and K. L. Narasimhan, *Phys. Rev. B*, 1999, **60**, 8246.
13 A. P. Alivisatos, *Science*, 1996, **271**, 933.
14 J. Chen, S. Shen, P. Guo, M. Wang, P. Wu, X. Wang and L. Guo, *Appl. Catal., B*, 2014, **152**, 335.
15 L. Kronik and Y. Shapira, *Surf. Interface Anal.*, 2001, **31**, 954.
16 L. Kronik and Y. Shapira, *Surf. Sci. Rep.*, 1999, **37**, 1.
17 J. Lagowski, *Surf. Sci.*, 1994, **299**, 92.
18 J. Zhao and F. E. Osterloh, *J. Phys. Chem. Lett.*, 2014, **5**, 782.
19 F. E. Osterloh, M. A. Holmes, J. Zhao, L. Chang, S. Kawula, J. D. Roehling and A. J. Moulé, *J. Phys. Chem. C*, 2014, **118**, 14723.

20 F. E. Osterloh, M. A. Holmes, L. Chang, A. J. Moulé and J. Zhao, *J. Phys. Chem. C*, 2013, **117**, 26905.
21 S. Ouyang, H. Tong, N. Umezawa, J. Cao, P. Li, Y. Bi, Y. Zhang and J. Ye, *J. Am. Chem. Soc.*, 2012, **134**, 1974.
22 D. J. Martin, K. Qiu, S. A. Shevlin, A. D. Handoko, X. Chen, Z. Guo and J. Tang, *Angew. Chem., Int. Ed.*, 2014, **53**, 9240.
23 J. Prabhuram and R. Manoharan, *J. Power Sources*, 1998, **74**, 54.
24 R. L. Chamousis and F. E. Osterloh, *Energy Environ. Sci.*, 2014, **7**, 736.
25 J. A. Singh, S. H. Overbury, N. J. Dudney, M. Li and G. M. Veith, *ACS Catal.*, 2012, **2**, 1138.
26 D. D. Perrin, *CRC Handbook of Chemistry and Physics*, CRC Press/Taylor and Francis, Boca Raton, FL, 2008.
27 E. Buncel and B. Menon, *J. Organomet. Chem.*, 1977, **141**, 1.

